ACS APPLIED MATERIALS & INTERFACES

Research Article

www.acsami.org

"Stainless" Gold Nanorods: Preserving Shape, Optical Properties, and SERS Activity in Oxidative Environment

Irene Vassalini,[†] Enzo Rotunno,[‡] Laura Lazzarini,[‡] and Ivano Alessandri*[,†]

[†]INSTM and Chemistry for Technologies Laboratory, Mechanical and Industrial Department, University of Brescia, Via Branze 38, 25123 Brescia, Italy

[‡]IMEM-CNR, Parco Area delle Scienze 37/A, 43124 Parma, Italy

Supporting Information

ABSTRACT: One of the main limitations to the application of gold nanorods (Au NRs) as surface-enhanced Raman scattering (SERS) probes for in situ monitoring of chemical processes is their instability in oxidative environments. Oxidation induces progressive anisotropic shortening of the NRs, which are eventually dissolved once this process has been completed. This paper compares two types of Au NRs, obtained through different routes and characterized by similar aspect ratios but different sizes. The key factors influencing the resistance of Au NRs to oxidation were systematically investigated, showing that the reduction of free bromide species and the increase of the particle size allowed the NRs to maintain their stability under harsh environments for several weeks. The most stable Au NRs were also demonstrated to be highly efficient SERS substrates in a series of Raman experiments involving molecular probes, treated under either oxidizing or nonoxidizing conditions, which simulate the oxidation of organic pollutants in water. These hallmarks make these "stainless" Au NRs attractive tools for ultrasensitive diagnostic under real working conditions.

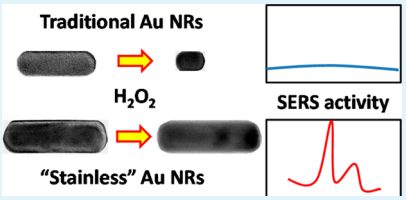

KEYWORDS: *gold nanorods, SERS, recyclable SERS materials, nanoparticle oxidation, organic pollutants, in situ Raman*

INTRODUCTION

Gold nanorods (Au NRs) are intensively investigated because of their large variety of applications in material science and theranostics.[1−5] Most of them rely on the exploitation of localized surface plasmon resonance (LSPR), which gives rise to a strong enhancement of the local electromagnetic field near the nanorod surface. Because of their anisotropic shape, the extinction spectrum of Au NRs exhibits two distinct LSPR peaks, corresponding to transverse and longitudinal plasmon modes.[6] The longitudinal peak is very intense, and its position can be finely tuned from the red to the near-infrared (NIR) spectral region, depending on the Au NR aspect ratio (AR), i.e., the ratio between length and width of the Au NRs.[7] The sensitivity to the AR has driven the development and optimization of advanced strategies for the synthesis of monodisperse Au NRs with longitudinal LSPR modes tailored to specific wavelengths.[8−11] Diameter is another important factor for controlling the optical properties of Au NRs.[12,13] Light absorption increases as diameter decreases, making Au NRs with diameters below 15 nm particularly efficient for plasmonic heating, with many potential applications in photothermal therapy and drug delivery.[14] On the other hand, as the diameter of Au NRs increases, light absorption decreases and scattering increases, making large Au NRs more suitable for surface-enhanced Raman spectroscopy (SERS) and bioimaging.[15,16] In this regard, Ye, Zheng, and co-workers have recently succeeded in producing highly monodisperse Au NRs, characterized by large diameters (>15 nm), which can efficiently scatter either Vis or NIR light.[17] This approach involves a binary surfactant mixture, based on the addition of sodium oleate (NaOL) to hexadecyltrimethylammonium bromide (CTAB), which is commonly used to direct the synthesis of Au NRs. NaOL plays a key role in the partial reduction of the gold precursor and mediates the binding between CTAB and the growing NRs.

The opportunity to optimize scattering and LSPR is challenging SERS to extend its range of applications to the detection of analytes under real working conditions.[18−20] In this regard, Au NRs must keep their size and shape in order to maintain their optical properties unaltered during a Raman experiment. This can be made difficult by the onset of unarrested growth phenomena, aggregation, or dissolution of the Au NRs in oxidative environments. Ligand exchange or polymer encapsulation have been successful in preventing uncontrolled growth and aggregation.[21−23] However, the maintenance of their optical properties under oxidative conditions has not been addressed so far. The oxidation potential of Au NRs (1.498 V vs normal hydrogen electrode (NHE) for the couple Au^{3+}/Au) shifts to lower values (0.854 V vs NHE)[24] in the presence of complexing bromide ions, originated from the excess of CTAB in solution, but, to date, oxidation has been considered as a tool to tune the optical properties of Au NRs.[25−30] For example, Ni et al. utilized hydrogen peroxide to obtain a controlled shortening of Au NRs along their main axis ([001] direction) as a function of the reaction time.[30]

Received: June 18, 2015
Accepted: August 10, 2015
Published: August 10, 2015

DOI: 10.1021/acsami.5b07175
ACS Appl. Mater. Interfaces 2015, 7, 18794−18802

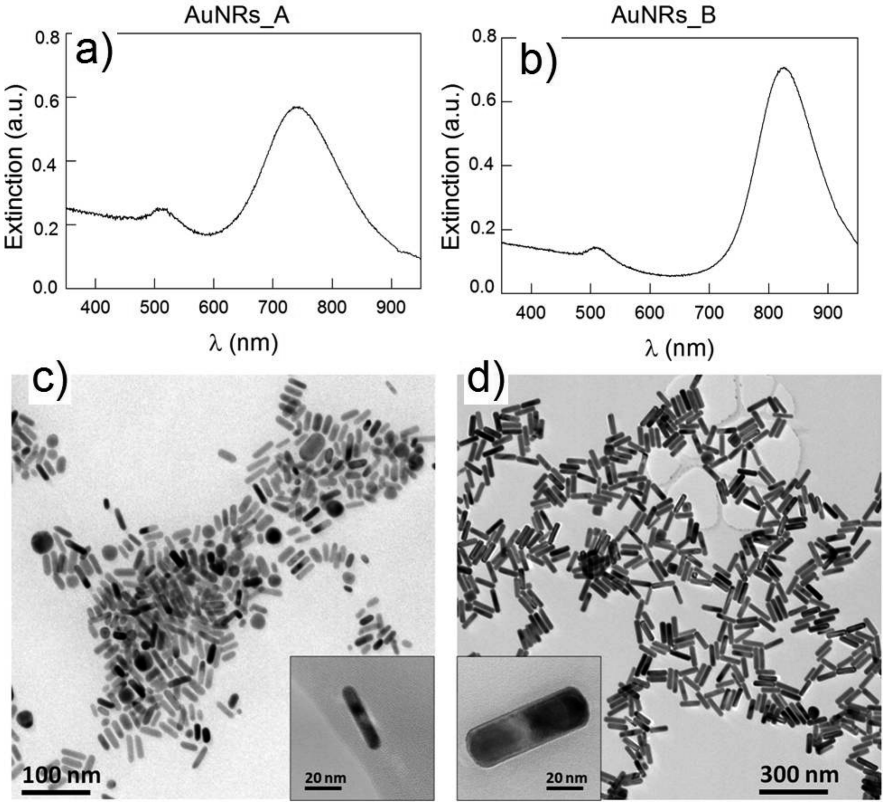

Figure 1. (Top) Optical extinction spectra of (a) as-synthesized Au NRs_A and (b) as-synthesized Au NRs_B. (Bottom) Representative TEM images of (c) as-synthesized AuNRs_A and (d) as-synthesized AuNRs_B.

However, the oxidation of Au NRs induces a progressive shift of the longitudinal LSPR peak, which decreases in intensity, broadens, and eventually disappears once all of thr Au nanoparticles have been dissolved. As a result, SERS activity can be strongly reduced or even lost. This prevents the use of AuNRs in monitoring most of the processes involving any analyte that can act as an oxidizing agent, including most of the reactive species taking part in cellular oxidative stress or oxidative removal of organic pollutants, like hydrogen peroxide ($E°$ H_2O_2/H_2O, H^+ = 1.776 V vs NHE), ozone ($E°$ O_3/O_2 = 2.076 V vs NHE). etc.[24] Thus, the synthesis of SERS-active Au NRs that can resist oxidation is a mandatory task that has not been addressed so far.

In this work, we compare the resistance to oxidation of two types of Au NRs, obtained through either traditional or binary-surfactant mixture routes. A careful control of the key parameters influencing the oxidation process (size of the NRs and concentration of the free Br^- ions) allowed the selection of Au NRs that can tolerate oxidative conditions without any modification of their optical properties. Their superior performance is demonstrated in a series of SERS experiments under oxidative conditions, in which the degradation of different organic dyes can be monitored through several detection cycles carried out on the same clusters of Au NRs.

EXPERIMENTAL SECTION

Materials. All chemicals were obtained from commercial suppliers and used without further purification. Hexadecyltrimethylammonium bromide (CTAB ≥ 99%), gold(III) chloride trihydrate ($HAuCl_4$ ≥ 99.9% trace metals basis), silver nitrate ($AgNO_3$, 99.9999% trace metals basis), L-ascorbic acid (99%), sodium borohydride ($NaBH_4$, 12 wt % solution in 14 M NaOH), hydrochloric acid (HCl, 37 wt % in water), potassium bromide (KBr, 99%), and hydrogen peroxide (H_2O_2, 35 wt % in water) were purchased from Sigma-Aldrich. Sodium oleate (NaOL > 97.0%) was purchased by TCI America.

Ultrapure water obtained from a Milli-Q Integral 5 system was used in all experiments. All glassware was cleaned using freshly prepared aqua regia, followed by rinsing with copious amounts of water.

Synthesis of Au NRs. Two different types of Au NRs (Au NRs_A and Au NRs_B) were synthesized and tested. They were prepared according to two different procedures.

Au NRs_A were obtained following the protocol proposed by Park et al.[44] The seed solution was prepared by mixing 5 mL of 0.2 M CTAB and 5 mL of 0.0005 M $HAuCl_4$ and by adding 600 μL of a freshly prepared, ice-cold 0.01 M $NaBH_4$ solution. The solution was stirred vigorously for 2 min, and it was aged for 5 min at 25 °C.

The growth solution was prepared separately, by mixing 10 mL of 0.2 M CTAB, 400 μL of 0.004 M $AgNO_3$, and 10 mL of 0.001 M $HAuCl_4$ at 25 °C. Next, 140 μL of 0.078 M ascorbic acid was added under stirring: the solution turned from light yellow to colorless. Finally, 24 μL of the seed solution aged for 5 min was added to the growth solution. The solution was kept at rest for at least 15 h at 25 °C.

Au NRs_B were prepared according to the procedure proposed by Ye et al.[17] Briefly, the seed solution was prepared by mixing 2 mL of 0.2 M CTAB and 2 mL of 0.0005 M $HAuCl_4$. $NaBH_4$ (400 μL, 0.002 M; freshly prepared but not ice-cold) was added. The solution was stirred vigorously for 2 min, and it was aged, without stirring, for 30 min at 25 °C.

The growth solution was prepared separately, by mixing 10 mL of a binary surfactant solution (obtained by dissolving 280 mg of CTAB (0.0768 M) and 49.4 mg of NaOL (0.0162 M)) with 720 μL of 0.004 M $AgNO_3$. The solution was kept at 30 °C for 15 min. Next, 10 mL of 0.001 M $HAuCl_4$ was added, and the solution was kept under mild stirring for 90 min at 30 °C. Then, 60 μL of 37% HCl in water was added, and the solution was kept under mild stirring for a further 15 min. Finally, 50 μL of 0.064 M ascorbic acid was added and stirred

DOI: 10.1021/acsami.5b07175
ACS Appl. Mater. Interfaces 2015, 7, 18794−18802

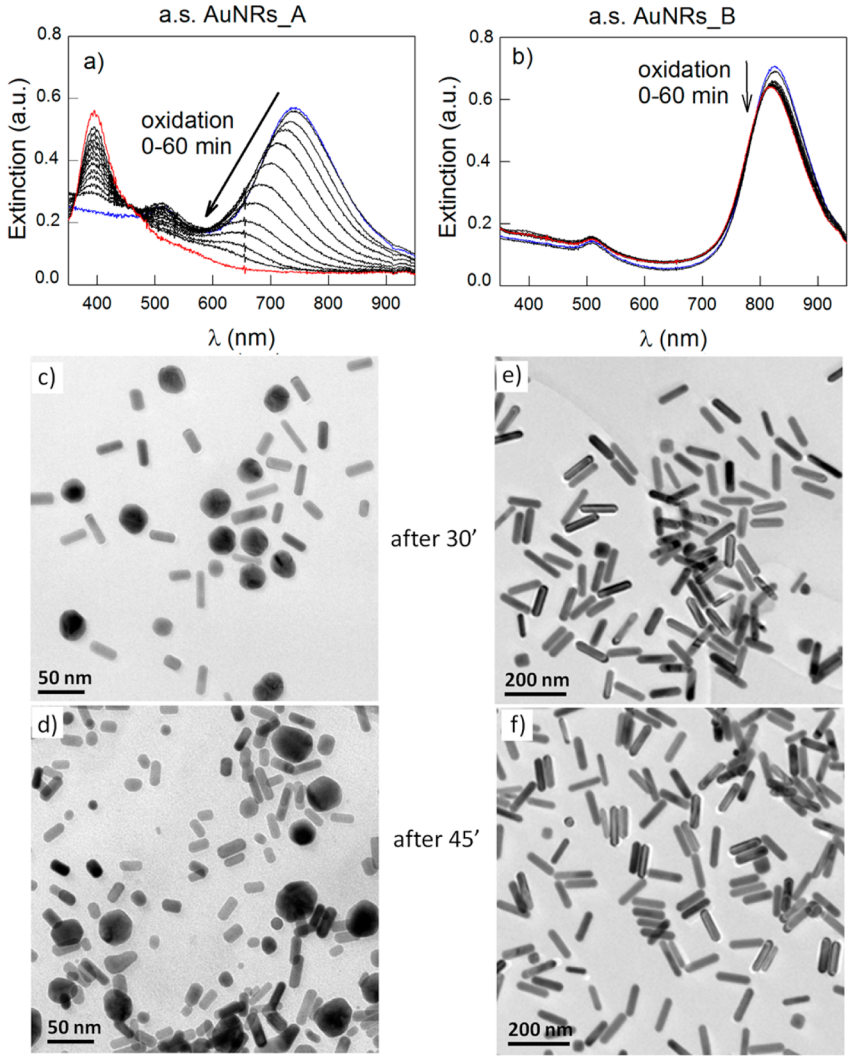

Figure 2. Oxidation of as-synthesized Au NRs. (Top) Evolution of the extinction spectra upon addition of H_2O_2 (a) Au NRs_A and (b) Au NRs_B. The spectra were taken every 5 min for 1 h. The blue line represents the starting sample. The red line shows the same sample after 1 h of reaction. (Bottom) TEM images of the Au NRs after 30 and 45 min from the addition of H_2O_2: (c, d) AuNRs_A and (e, f) AuNRs_B.

vigorously for 30 s, and 16 μL of the seed solution aged for 30 min was incorporated. The solution was stirred for 30 s, and it was kept at rest at 25 °C for at least 15 h. Different batches of Au NRs_B were prepared with AR ranging from about 3.5:1 to 4.3:1.

Oxidation Tests. The study of the Au NRs resistance in oxidizing environment was performed as follows: 1 mL of AuNRs suspension was mixed at room temperature with 100 μL of 35 wt % H_2O_2 solution. To optimize the H_2O_2 oxidizing activity, the pH of the suspensions has to be included between 3 and 4 by adjusting with HCl or NaOH, when necessary.

For further characterizations, portions of both types of Au NRs were centrifuged and resuspended in water, 0.1 M CTAB solution, or 0.1 M KBr solution. Centrifugation was carried out twice at 7000 rpm for 15 min.

Characterization. *UV–Vis–NIR Spectroscopy.* The extinction spectra of the Au NRs were acquired by a UV–vis–NIR spectrophotometer (QE 65000 Ocean Optics). The original solution of Au NRs_B was diluted with Milli-Q water to make the intensity of extinction spectra comparable to that of Au NRs_A.

Raman Microspectroscopy. The Raman characterization was carried out by a high-resolution Raman microspectrometer (Labram HR-800, Horiba Jobin-Yvon) using a He–Ne laser source (λ = 632.8 nm). All the spectra were acquired in backscattering mode, using a 100× (Numerical Aperture: 0.9) microscope objective to focus and collect the exiting light. Different concentrations (from 10^{-3} to 10^{-8} M) of crystal violet (CV, tris(4-(dimethylamino)phenyl)methylium chloride) and methylene blue (MB, 3,7-bis(dimethylamino)-phenothiazin-5-ium chloride) aqueous solutions were used as molecular probes to test the SERS performances of the Au NRs. Both types of Au NR solutions with the same optical density were incubated with CV (MB) for 30 min, centrifuged, and resuspended in Milli-Q water. In both cases, Au NRs that had reacted with H_2O_2 for 1 h were tested as well.

The different Au NR–CV (–MB) solutions (5 μL) were dropped on glass microscope slides for Raman analysis. Reference spectra were acquired by dropping 5 μL of CV or MB solution at different concentrations on a glass microscope slide. Upon drying at room temperature, each sample was analyzed by measuring different regions of the substrate. All the selected areas were optically clean; optically visible agglomerates of CV (MB) were not considered in sampling. The study of CV and MB oxidation was carried out by dropping 5 μL of 35 wt % H_2O_2 onto the previously measured samples.

Transmission Electron Microscopy Analyses. Transmission electron microscopy (TEM) observations were carried out by means of a high-resolution, (0.18 nm) field-emission JEOL 2200FS microscope, equipped with in-column Ω energy filter, 2 high-angle annular dark-field (HAADF) detectors, and X-ray microanalysis (EDS). Samples were prepared by dispersing a few drops of the NR solution on holey carbon grids and drying them in air.

DOI: 10.1021/acsami.5b07175
ACS Appl. Mater. Interfaces 2015, 7, 18794–18802

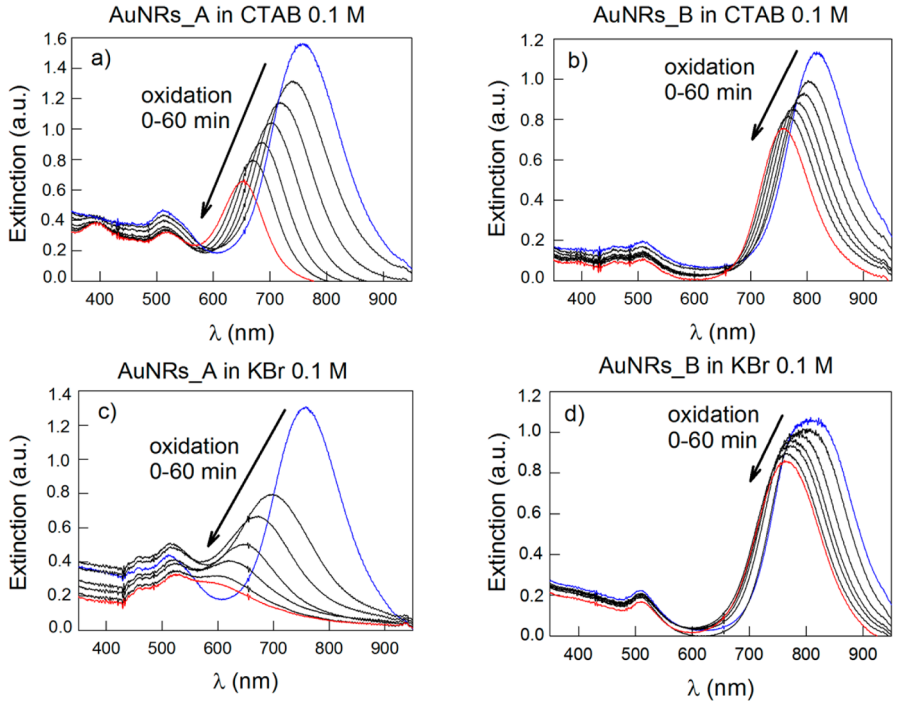

Figure 3. Optical extinction of Au NRs centrifuged and resuspended either in 0.1 M CTAB (top) or KBr (bottom) solutions upon addition of H_2O_2: (a, c) AuNRs_A and (b, d) AuNRs_B. In all cases, the spectra were taken every 10 min for 1 h. The blue line represents the starting sample, and the red line represents the sample after 1 h of reaction.

Total Reflection X-ray Fluorescence. Total reflection X-ray fluorescence (TXRF) measurements were performed with the Bruker TXRF system S2 Picofox (air-cooled, Mo tube, silicon-drift detector), with operating values of 50 kV and 750 mA, using an acquisition time of 600 s.

RESULTS AND DISCUSSION

This work investigates the capability of Au NRs to maintain their optical properties under oxidative conditions, in view of their possible application in SERS experiments involving oxidizing agents. We focused our attention on two different types of Au NRs: Au NRs_A and Au NRs_B.

Au NRs_A were synthesized through a traditional approach, using 0.1 M CTAB solution as a surfactant, for directing growth and stabilizing the resulting nanostructures (see Experimental Section). These Au NRs exhibit their characteristic longitudinal LSPR peak at ~735 nm (Figure 1a). TEM analysis (Figure 1c) shows that the AR is ~3.8:1, resulting from the ratio between average lengths of 32 ± 8 nm and diameters of 8.5 ± 2 nm (see Supporting Information, Figure SI1).

On the other hand, Au NRs_B were synthesized using a binary surfactant mixture of NaOL and CTAB (see Experimental Section). In comparison to the traditional approach, here the concentration of CTAB in the growth solution is reduced to 0.0384 M and NaOL is exploited to achieve Au NRs with larger sizes, according to the mechanism proposed by Murray and co-workers.[17,31] Different ARs can be obtained through a simple modification of the synthesis protocol.[32] The maximum extension of the longitudinal LSPR peak for the Au NRs_B considered in this work was ~825 nm (Figure 1b). On the basis of TEM analysis (Figure 1d), the average length and diameter of these Au NRs_B are 89 ± 18 and 21 ± 3 nm, respectively (see Figure SI1). Thus, their AR (4.3:1) is slightly higher yet comparable to that of the Au NRs_A samples. Such a larger size results from the use of NaOL, which acts as both a protecting and a reducing agent, allowing to slow down and control the overgrowth process.[17] In particular, their larger average diameter makes Au NRs_B more efficient than Au NRs_A as light scatterers.

Both Au NRs were tested under oxidative conditions by studying the extinction spectra of the original Au NR solutions, with a comparable optical density, as a function of time upon addition of a 35 wt % H_2O_2 solution, as oxidizing agent, in 1:10 volume ratio with respect to the Au NR solution.

Figure 2 shows the comparison between the optical extinction spectra of the two types of Au NRs over a time scale extended up to 1 h from H_2O_2 addition. Within this lapse of time, the longitudinal LSPR peak of Au NRs_A undergoes a progressive blue-shift and broadening (Figure 2a), as a result of the uniaxial shortening, occurring upon oxidation. This peak blue-shift proceeds at ~2.5 nm/min (Figure 2c), before merging with transverse mode into a single LSPR broad peak, typical of spheroidal nanoparticles. These data support the hypothesis of an uniaxial shortening, with Au(0) that dissolves starting from the nanorod tips, which are less protected by the capping agents. TEM images acquired after 30 and 45 min (Figure 2c and 2d) witness this evolution, showing an ever-increasing number of spheroids as a function of time. These spheroids originate from the aggregation of small particles, resulting from the nanorod shortening. The reduction of the average AR from 3.8:1 (before H_2O_2) to 2.2:1 (after 45 min from H_2O_2 addition) is a direct indication of the transformation of the NRs into nanospheroids (see Figure SI1).

When the oxidation process is completed, any LSPR peak disappears, as a consequence of the total dissolution of Au, which has been converted into $AuBr_4^-$, according to the following overall reaction:

$$2Au + 3H_2O_2 + 8Br^- + 6H^+ \rightarrow 2[AuBr_4]^- + 6H_2O \quad (1)$$

DOI: 10.1021/acsami.5b07175
ACS Appl. Mater. Interfaces 2015, 7, 18794−18802

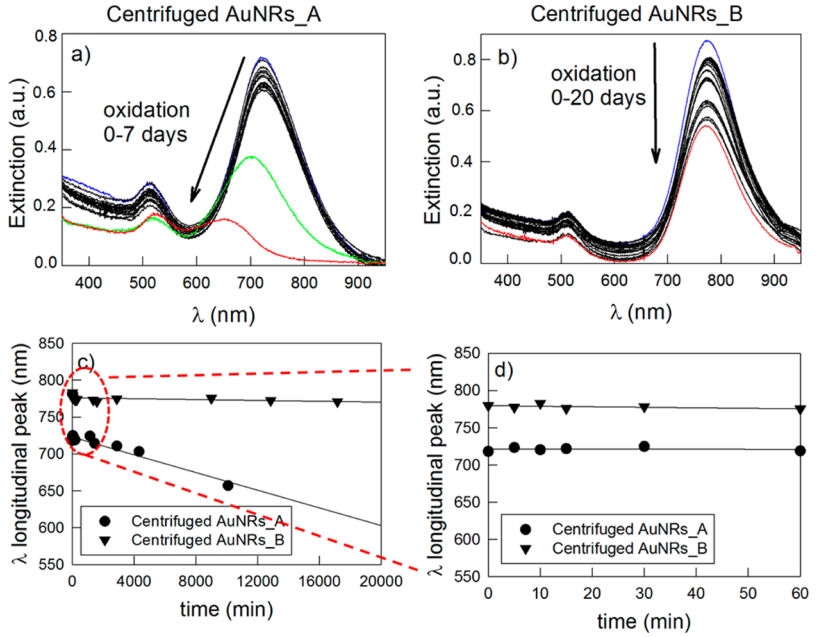

Figure 4. Oxidation of centrifuged Au_NRs upon addition of H_2O_2 without any extra-source of free Br^- ions. Optical extinction of (a) Au_NRs_A and (b) Au_NRs_B samples. (a) Blue line represents the starting sample, green line represents the sample after 3 days of reaction, and red line represents the sample after 7 days. (b) Blue line represents the starting sample, while red line represents the sample after 20 days. (c) Variation of the position of the longitudinal LSPR peak as a function of time, over 2 weeks. (d) Zoom on data referred to the first hour of reaction.

The formation of $AuBr_4^-$ gives rise to the peak at 390 nm, corresponding to the ligand-to-metal charge transfer (LMCT) signal of $[CTA]^+[AuBr_4]^-$ complex,[33] which progressively grows as the oxidation proceeds. These results fully agree with those reported by other research groups for the oxidation of analogous systems.[29,30]

On the contrary, the position of the longitudinal LSPR peak of Au NR_B does not change in the same period of time (Figure 2b). TEM analysis confirms that the structure of these nanorods is not significantly affected by the addition of H_2O_2 (Figure 2e and 2f). These results indicate that, within 1 h, which can be considered as a reasonable period of time for a dynamic Raman experiment, Au NRs_B are stable against oxidation and do not modify their optical properties. Following this system for an extended period of time, we can observe the onset of a significant blue-shift only after 4 h, yet their oxidation is not completed even after 24 h (see Figure SI2). A direct comparison of extinction spectra and LSPR shift between Au NRs with the same AR is reported in Figure SI3, showing the same trend discussed earlier.

Au NRs_B solutions are characterized by a reduced amount of CTAB (see also TXRF analysis, Figure SI4). Rodríguez-Fernández et al. proposed that the anisotropic shortening of gold nanorods in an oxidizing environment is mediated by CTAB micelles, which are expected to trap the gold ions resulting from oxidation. The higher reactivity of nanorod tips has been ascribed to a higher probability of collision with micelles.[26] On the other hand, CTAB can be more simply regarded as a source of Br^- ions, which are essential to complex the gold ions and drive the oxidation reaction.

To gain more insight into this issue, two further experiments were carried out. In the first one, both Au NR solutions were centrifuged and resuspended in a 0.1 M CTAB solution. Figure 3a and 3b show the evolution of the extinction spectra of both types of NRs in the first hour after the addition of H_2O_2. The oxidation rate of Au NRs_B (Figure 3b) is significantly enhanced in comparison to the original solution, indicating that the excess of CTAB has a detrimental effect on the resistance to oxidation. Nevertheless, Au NRs_A are still less stable against oxidation than Au NRs_B (Figure 3a).

In the second experiment, the evolution of the optical extinction spectra upon addition of H_2O_2 was monitored for both pristine NR samples, each one previously centrifuged and resuspended in a 0.1 M KBr solution, without any further addition of CTAB (Figure 3c and 3d). Again, upon addition of H_2O_2, both Au NR solutions are oxidized, although Au NRs_B are still more stable than Au NRs_A.

These results suggest that surfactant micelles are not necessary to drive anisotropic shortening of Au NRs. Anisotropic shortening is inherently related to the higher reactivity of the less-protected nanorods tips, which has been widely documented in literature,[25−30] and it is associated with their higher accessibility. On the other hand, the presence of complexing Br^- ions, either from CTAB or KBr, is the real key factor for promoting oxidation. This is confirmed by the high oxidation rate of Au NRs_A original solutions, which is related to the high concentration of Br^- ion sources (CTAB), as well as by the increased oxidation rate of Au NRs_B, upon addition of either CTAB or KBr. Moreover, Zhu et al. have recently demonstrated that Br^- is directly oxidized by hydrogen peroxide to Br_2, which is in turn converted into Br_3^- in the presence of Br^- species, resulting in the oxidation of gold.[29]

Thus, to increase the stability of Au NRs in an oxidizing environment, any source of Br^- ions should be removed or, at least, minimized. To demonstrate this hypothesis, a new series of experiments were carried out, in which the stability of the Au NRs against oxidation was tested without any bromide in excess. To obtain this condition, both Au NR original solutions were centrifuged and resuspended in Milli-Q water, upon removal of supernatant species. Figure 4 shows the extinction spectra of the Au NR solutions. The absence of Br^- ions

DOI: 10.1021/acsami.5b07175
ACS Appl. Mater. Interfaces 2015, 7, 18794−18802

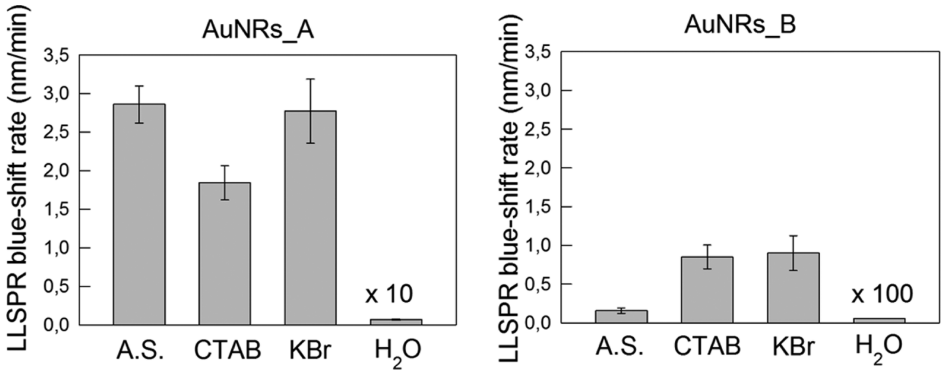

Figure 5. Comparative summary of the oxidation rates obtained by monitoring the blue-shift of the longitudinal LSPR peak for AuNRs_A and AuNRs_B samples under different conditions: as-synthesized (A.S.); after centrifugation and resuspension in 0.1 M CTAB solution (CTAB); after centrifugation and resuspension in 0.1 M KBr solution (KBr); and after centrifugation and resuspension in water (H_2O).

contributes to remarkably improve the stability of both types of nanorods (see also Figure SI5).

Au NRs_A remain stable up to 2 days, whereas Au NRs_B do not significantly change their spectrum within 20 days. These data confirm the importance of complexing Br^- ions in lowering the oxidation potential of gold, which resembles the role played by Cl^- in aqua regia solutions.

Figure 5 summarizes the results of all the experiments discussed earlier, giving a quantitative evaluation of the oxidation rate under different conditions, in terms of longitudinal LSPR peak blue-shift as a function of time. Although the general trend of stability is analogous for both systems and clearly indicates the key role of Br^- ions in controlling oxidation, it should be noted that Au NRs_B are systematically more stable than Au NRs_A, even when the overall concentration of Br^- ions is the same for both samples.

The higher stability of Au NRs_B can be caused by several factors, related to their differences in comparison to the traditional Au NRs_A obtained through the CTAB route. The clearest difference is that Au NRs_B are bigger than Au NRs_A. This means that, in the case of Au NRs_B, there are many more atoms that should be oxidized and released from unprotected tips before any significant modification of the AR can be observed. This might explain the difference of 1 order of magnitude in oxidation rate between types A and B centrifuged samples. Au NRs_B do not exhibit any preferred orientation of the crystalline planes (e.g., the octagonal facets typical of Au NRs synthesized using bromide-free surfactants)[31,32] in comparison to the A counterpart (see Figure SI6). Thus, the possibility of a different reactivity of the Au surface cannot be considered as a key factor to explain the highest resistance of Au NRs_B. On the other hand, the different accessibility of free Br^- ions to the Au surface is expected to influence the oxidation rate. A more detailed investigation on the role of NaOL in affecting the efficiency of complexation of Br^- ions is currently underway.

As our interest in Au NRs_B is focused on the possibility to use them as oxidation-resistant SERS substrates, we tested their SERS activity in detection of organic dyes that are commonly used as molecular probe in SERS experiments, such as crystal violet (CV) and methylene blue (MB).[34]

In this regard, we should recall that Raman response is strongly dependent on the number and reciprocal orientation of Au NRs that are aggregated to form SERS-active substrates.[35] In the present case, all the Raman spectra were carried out on randomly oriented small agglomerates formed by 3−6 Au NRs (see Figure SI7). Figure 6 shows the Raman spectra of CV solutions at different concentrations (5×10^{-5}−10^{-8} M) acquired using Au NRs_B (see Experimental Section). The spectrum of a 10^{-3} M CV solution acquired without NRs is shown as a reference. This corresponds to the detection limit of CV for normal Raman acquisition under the same conditions. These data show that Au NRs_B can be used as efficient SERS substrates. Details on the calculations of the enhancement factor are reported in Figure SI8. A simple, rough estimate of the analytical enhancement factor (AEF) gives average values of the order of $\sim 10^4$ for different peaks taken as a reference (e.g., 925 and 1622 cm^{-1}, corresponding to the $\delta C-C_{center}-C$ 17_a bending- and 8_a stretching-modes of benzene rings, respectively),[36] which accounts for the extension of the detection limit of 4 orders of magnitude in the presence of Au NRs_B. A more accurate, yet approximate, evaluation, based on the definition of SERS substrate enhancement factor (SSEF),[37] which accounts for the number of molecules adsorbed on the SERS-active surface, further increases these values to $\sim 10^6$−10^7 (see Figure SI8).

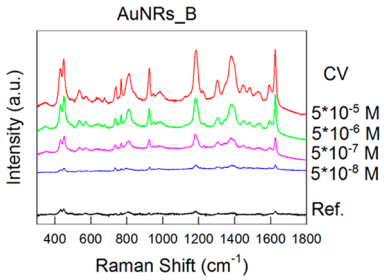

Figure 6. Raman spectra of crystal violet (CV) solutions of different concentrations, using AuNRs_B as SERS enhancers. The spectrum of a CV 10^{-3} M solution is reported as reference. All the spectra were acquired using a 100× (NA: 0.9) objective. Acquisition time: 5 s.

The most interesting point is related to the possibility to directly compare the SERS efficiency of both types of Au NRs, under either normal conditions or oxidative environment (e.g., after their reaction with H_2O_2 for 1 h). This comparison, carried out using the same concentration (5×10^{-6} M) and amount of CV solution, is shown in Figure 7. Au NRs_B outperform their A counterparts in both cases. They are more efficient SERS substrates under normal conditions, with the average intensity I_{AuNRs_B}/I_{AuNRs_A} ratio of the main peaks ranging between 16 and 18. This could be expected as a result

DOI: 10.1021/acsami.5b07175
ACS Appl. Mater. Interfaces 2015, 7, 18794−18802

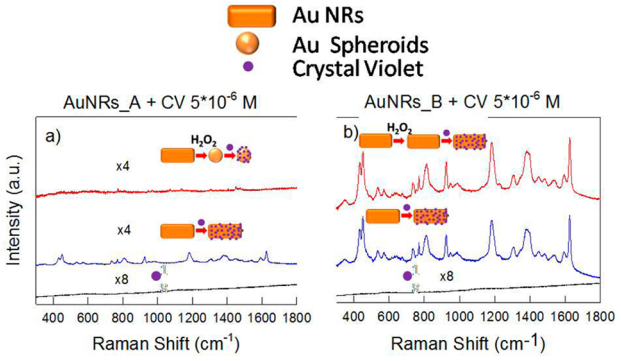

Figure 7. Raman spectra of 5×10^{-6} M crystal violet solution, using (a) AuNRs_A and (b) AuNRs_B as SERS-active substrates. In both cases, the black line is related to a reference 10^{-5} M CV solution dropped on a glass slide without any SERS substrates. The blue line is related to the 5×10^{-6} M CV solution, using as-synthesized Au NRs as SERS-active substrates. The red line is related to the 5×10^{-6} M CV solution, adsorbed onto as-synthesized Au NRs previously treated with H_2O_2 for 1 h. All the spectra were acquired using a 100× (NA: 0.9) objective.

of their larger size, which makes them more efficient in light scattering, confirming the hypotheses made by Murray and coworkers.[17]

However, the most remarkable result is observed under oxidative conditions. As expected from the previous experiments on extinction spectra, we found out that Au NRs_A treated with H_2O_2 for 1 h are no more active as SERS substrates, as a consequence of their complete oxidation, which determines the complete disappearance of their plasmonic bands. Thus, they could not be utilized in experiments involving an oxidative environment, because of the loss of their stability during the Raman experiment. On the other hand, Au NRs_B exhibit unaltered SERS activity under oxidative conditions. These results mirror the trend of bulk optical properties discussed before, highlighting the opportunity to exploit this superior resistance to oxidation for SERS experiments under harsh environments.

As a proof-of-concept, AuNRs_B were tested as SERS substrates for monitoring the degradation of CV, upon the addition of H_2O_2. Figure 8a shows the SERS monitoring of five detection/removal cycles for a 5×10^{-6} M CV solution adsorbed on Au NRs_B. The Raman spectrum of CV, which is clearly observed before addition of H_2O_2, vanishes upon H_2O_2 treatment, as a consequence of the dye degradation. When a new droplet of the CV solution is added on the same SERS-active region, the Raman spectrum is fully recovered, demonstrating that Au NRs_B maintain their optical activity during H_2O_2 treatment. This cycle can be repeated many times (our tests were limited to 10 cycles), without showing any significant loss of SERS activity. These results demonstrate that Au NRs_B can be successfully used for monitoring a variety of oxidation reactions, as those used in many environmental remediation processes, because their stability allows for correlating any changes in the spectrum of the analyte to oxidative processes occurring on the analyte itself. The concept of oxidation-resistant, recyclable, SERS-active substrates could be very useful in view of comparing the relative rates of oxidation reactions for different analytes.[38,39] Figure 8b shows an example of the alternate detection of two organic dyes (CV and MB), through the same detection/removal cycles described above. Upon the complete removal of the first analyte (e.g., CV), another analyte (e.g., MB) can be detected and

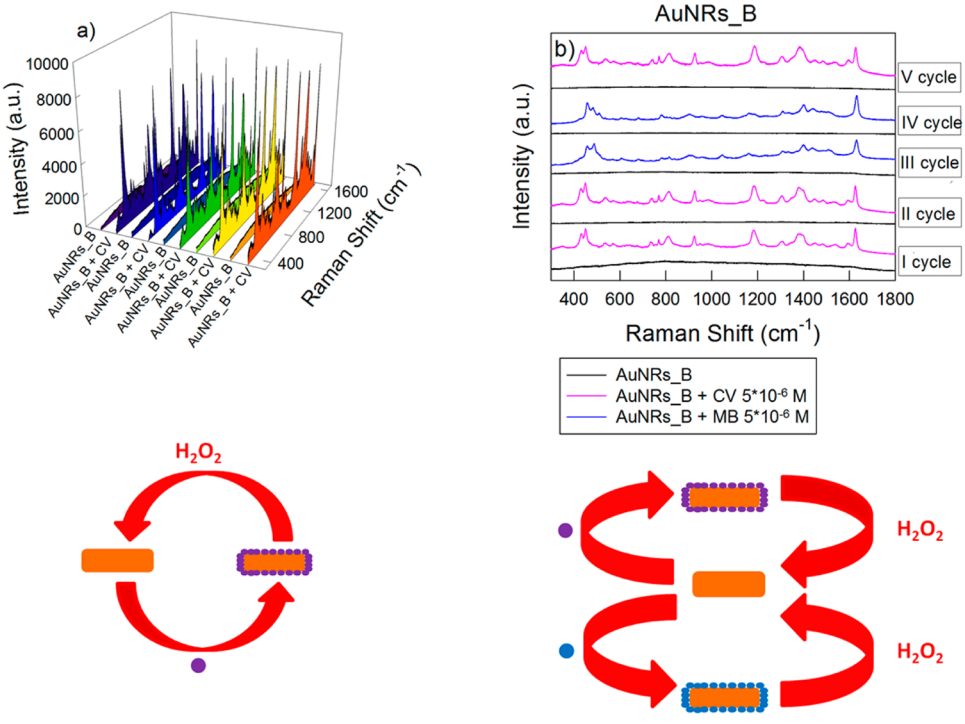

Figure 8. AuNRs_B as recyclable SERS substrates. (a) Detection/removal cycles for a 5×10^{-6} M CV solution analyzed before and after addition of H_2O_2. H_2O_2 removes CV without altering the optical properties of the Au NRs_B, which are reused for the analysis of other solutions. (b) Alternate detection/removal cycles of 5×10^{-6} M CV (fuchsia spectra) and MB (blue spectra) solutions obtained on the same aggregates of Au NRs_B samples. All the spectra were acquired using a 100× (NA: 0.9) objective. Acquisition time: 5 s.

DOI: 10.1021/acsami.5b07175
ACS Appl. Mater. Interfaces 2015, 7, 18794−18802

subsequently removed, with the interesting opportunity to compare two or more processes occurring exactly at the same place. This represents a major advancement in the use of Au NRs as SERS-active probes for monitoring chemical reactions and processes under real working conditions.

Further improvements might be achieved by controlling the aggregation of AuNRs used as SERS-active substrates through end-to-end functionalization[40,41] or template-mediated assembly.[42] Finally, the resistance to oxidation of these Au NRs can be exploited not only for SERS but also in LSPR-based and single-molecule fluorescence experiments.[43]

CONCLUSION

This work demonstrates that, in the case of Au NRs used for SERS applications, size plays a key role not only in determining the Raman response but also in controlling resistance to oxidation. A systematic investigation of the oxidation rate of Au NRs revealed that the concentration of Br^- ions is a critical factor for controlling the overall process and, in general, Au NRs are made more stable when the amount of Br^- species is reduced. We have also demonstrated that Au NRs with high SERS efficiency can be obtained through synthetic routes that are alternative to the conventional ones. In particular, the use of NaOL as surfactant/reducing agent in a binary mixture with CTAB leads to high-quality, large Au NRs, which exhibit improved light scattering and SERS activity. These NRs maintain their shape and optical properties under strongly oxidizing conditions, allowing for detection of different types of analytes and monitoring of their reactivity on selected sites in real time. These results open interesting perspectives for in situ experiments needing stable, ultrasensitive SERS platforms for investigating chemical reactions involving strongly oxidizing species, such as the processes for environmental remediation.

ASSOCIATED CONTENT

Supporting Information

The Supporting Information is available free of charge on the ACS Publications website at DOI: 10.1021/acsami.5b07175.

Additional TEM images, descriptive statistics of size and aspect ratio, extinction UV−vis−NIR spectra of Au NRs_A and Au NRs_B over prolonged periods, TXRF and STEM-HAADF analysis, and details on the evaluation of enhancement factors (PDF)

AUTHOR INFORMATION

Corresponding Author

*ivano.alessandri@unibs.it.

Notes

The authors declare no competing financial interest.

ACKNOWLEDGMENTS

This project has been partially supported by Supranano (INSTM-Regione Lombardia Project).

REFERENCES

(1) Halas, N. J.; Lal, S.; Chang, W. S.; Link, S.; Nordlander, P. Plasmons in Strongly Coupled Metallic Nanostructures. *Chem. Rev.* **2011**, *111*, 3913−3961.

(2) Perez-Juste, J.; Pastoriza-Santos, L.; Liz-Marzán, L. M.; Mulvaney, P. Gold Nanorods: Synthesis, Characterization and Applications. *Coord. Chem. Rev.* **2005**, *249*, 1870−1901.

(3) Huang, X.; Neretina, S.; El-Sayed, M. a. Gold Nanorods: From Synthesis and Properties to Biological and Biomedical Applications. *Adv. Mater.* **2009**, *21*, 4880−4910.

(4) Dykman, L.; Khlebtsov, N. Gold Nanoparticles in Biomedical Applications: Recent Advances and Perspectives. *Chem. Soc. Rev.* **2012**, *41*, 2256−2282.

(5) Smith, B. E.; Roder, P. B.; Zhou, X.; Pauzauskie, P. J. Nanoscale Materials for Hyperthermal Theranostics. *Nanoscale* **2015**, *7*, 7115−7126.

(6) Chen, H.; Shao, L.; Li, Q.; Wang, J. Gold Nanorods and Their Plasmonic Properties. *Chem. Soc. Rev.* **2013**, *42*, 2679−2724.

(7) Skirtach, A. G.; Karageorgiev, P.; De Geest, B. G.; Pazos-Perez, N.; Braun, D.; Sukhorukov, G. B. Nanorods as Wavelength-Selective Absorption Centers in the Visible and Near-Infrared Regions of the Electromagnetic Spectrum. *Adv. Mater.* **2008**, *20*, 506−510.

(8) Nikoobakht, B.; El-Sayed, M. a. Preparation and Growth Mechanism of Gold Nanorods (NRs) Using Seed-Mediated Growth Method. *Chem. Mater.* **2003**, *15*, 1957−1962.

(9) Sau, T. K.; Murphy, C. J. Seeded High Yield Synthesis of Short Au Nanorods in Aqueous Solution. *Langmuir* **2004**, *20*, 6414−6420.

(10) Lohse, S. E.; Murphy, C. J. The Quest for Shape Control: A History of Gold Nanorod Synthesis Metal "Whiskers" Photochemical/(VLS) Electrochemical Seeded Growth. *Chem. Mater.* **2013**, *25*, 1250−1261.

(11) Sau, T. K.; Rogach, A. L. Nonspherical Noble Metal Nanoparticles: Colloid-Chemical Synthesis and Morphology Control. *Adv. Mater.* **2010**, *22*, 1781−1804.

(12) Lee, K.-S.; El-Sayed, M. A. Dependence of the Enhanced Optical Scattering Efficiency Relative to that of Absorption for Gold Metal Nanorods on Aspect Ratio, Size, End-Cap Shape and Medium Refractive Index. *J. Phys. Chem. B* **2005**, *109*, 20331−20338.

(13) Brioude, A.; Jiang, X. C.; Pileni, M. P. Optical Properties of Gold Nanorods: DDA Simulations Supported by Experiments. *J. Phys. Chem. B* **2005**, *109*, 13138−13142.

(14) Wijaya, A.; Schaffer, S. B.; Pallares, I. G.; Hamad-Schifferli, K. Selective Release of Multiple DNA Oligonucleotides from Gold Nanorods. *ACS Nano* **2009**, *3*, 80−86.

(15) von Maltzahn, G.; Centrone, A.; Park, J.-H.; Ramanathan, R.; Sailor, M. J.; Hatton, T. A.; Bhatia, S. N. SERS-Coded Gold Nanorods as Multifunctional Platform for Densely Multiplexed Near-Infrared Imaging and Photothermal Heating. *Adv. Mater.* **2009**, *21*, 3175−3180.

(16) Jain, P. K.; Lee, K. S.; El-Sayed, I. H.; El-Sayed, M. a. Calculated Absorption and Scattering Properties of Gold Nanoparticles of Different Size, Shape, and Composition: Applications in Biological Imaging and Biomedicine. *J. Phys. Chem. B* **2006**, *110*, 7238−7248.

(17) Ye, X.; Zheng, C.; Chen, J.; Gao, Y.; Murray, C. B. Using Binary Surfactant Mixtures to Simultaneously Improve the Dimensional Tunability and Monodispersity in the Seeded Growth of Gold Nanorods. *Nano Lett.* **2013**, *13*, 765−771.

(18) Alessandri, I. Enhancing Raman Scattering without Plasmons: Unprecedented Sensitivity Achieved by TiO_2 Shell-Based Resonators. *J. Am. Chem. Soc.* **2013**, *135*, 5541−5544.

(19) Alessandri, I.; Depero, L. E. All-Oxide-Active Traps for Light and Matter: Probing Redox Homeostasis Model Reactions in Aqueous Environment. *Small* **2014**, *10*, 1294−1298.

(20) Salmistraro, M.; Schwartzberg, A.; Bao, W.; Depero, L. E.; Weber-Bargioni, A.; Cabrini, S.; Alessandri, I. Triggering and Monitoring Plasmon-Enhanced Reactions by Optical Nanoantennas Coupled to Photocatalytic Beads. *Small* **2013**, *9*, 3301−3307.

(21) Vigderman, L.; Manna, P.; Zubarev, E. R. Quantitative Replacement of Cetyl Trimethylammonium Bromide by Cationic Thiol Ligands on the Surface of Gold Nanorods and Their Extremely Large Uptake by Cancer Cells. *Angew. Chem., Int. Ed.* **2012**, *51*, 636−641.

(22) Zweifel, D. A.; Wei, A. Sulfide-Arrested Growth of Gold Nanorods. *Chem. Mater.* **2005**, *17*, 4256−4261.

(23) Kim, D. H.; Wei, A.; Won, Y. Preparation of Super-Stable Gold Nanorods via Encapsulation into Block Copolymer Micelles. *ACS Appl. Mater. Interfaces* **2012**, *4*, 1872−1877.

DOI: 10.1021/acsami.5b07175
ACS Appl. Mater. Interfaces 2015, 7, 18794−18802

(24) Vanysek, P. Electrochemical Series. In *CRC Handbook of Chemistry and Physics*, internet version 2005; Lide, D. R., Ed.; CRC Press: Boca Raton, FL, 2005; pp 8.20−8.29.
(25) Jana, N. R.; Gearheart, L.; Obare, S. O.; Murphy, C. J. Anisotropic Chemical Reactivity of Gold Spheroids and Nanorods. *Langmuir* **2002**, *18*, 922−927.
(26) Rodríguez-Fernández, J.; Pérez-Juste, J.; Mulvaney, P.; Liz-Marzán, L. M. Spatially-Directed Oxidation of Gold Nanoparticles by Au(III)−CTAB Complexes. *J. Phys. Chem. B* **2005**, *109*, 14257−14261.
(27) Tsung, C. K.; Kou, X.; Shi, Q.; Zhang, J.; Yeung, M. H.; Wang, J.; Stucky, G. D. Selective Shortening of Single-Crystalline Gold Nanorods by Mild Oxidation. *J. Am. Chem. Soc.* **2006**, *128*, 5352−5353.
(28) Chandrasekar, G.; Mougin, K.; Haidara, H.; Vidal, L.; Gnecco, E. Shape and Size Transformation of Gold Nanorods (GNRs) via Oxidation Process: A Reverse Growth Mechanism. *Appl. Surf. Sci.* **2011**, *257*, 4175−4179.
(29) Zhu, Q.; Wu, J.; Zhao, J.; Ni, W. Role of Bromide in Hydrogen-Peroxide Oxidation of CTAB-Stabilized Gold Nanorods in Aqueous Solutions. *Langmuir* **2015**, *31*, 4072−4077.
(30) Ni, W.; Kou, X.; Yang, Z.; Wang, J. Tailoring Longitudinal Surface Plasmon Wavelengths, Scattering and Absorption Cross Sections of Gold Nanorods. *ACS Nano* **2008**, *2*, 677−686.
(31) Ye, X.; Gao, Y.; Chen, J.; Reifsnyder, D. C.; Zheng, C.; Murray, C. B. Seeded Growth of Monodisperse Gold Nanorods Using Bromide-Free Surfactant Mixtures. *Nano Lett.* **2013**, *13*, 2163−2171.
(32) Khlebtsov, B. N.; Khanadeev, V. a.; Ye, J.; Sukhorukov, G. B.; Khlebtsov, N. G. Overgrowth of Gold Nanorods by Using a Binary Surfactant Mixture. *Langmuir* **2014**, *30*, 1696−1703.
(33) Kundu, S. A New Route for the Formation of Au Nanowires and Application of Shape-Selective Au Nanoparticles in SERS Studies. *J. Mater. Chem. C* **2013**, *1*, 831−842.
(34) Kneipp, J.; Kneipp, H.; Rajadurai, A.; Redmond, R. W.; Kneipp, K. Optical Probing and Imaging of Live Cells Using SERS Labels. *J. Raman Spectrosc.* **2009**, *40*, 1−5.
(35) Pal, S. K.; Depero, L. E.; Alessandri, I. Using Aggregates of Gold Nanorods in SER(R)S Experiments: An Empirical Evaluation of Some Critical Aspects. *Nanotechnology* **2010**, *21*, 425701.
(36) Cañamares, M. V.; Chenal, C.; Birke, R. L.; Lombardi, J. R. DFT, SERS, and Single-Molecule SERS of Crystal Violet. *J. Phys. Chem. C* **2008**, *112*, 20295−20300.
(37) Le Ru, E. C.; Blackie, E.; Meyer, M.; Etchegoin, P. G. Surface Enhanced Raman Scattering Enhancement Factors: A Comprehensive Study. *J. Phys. Chem. C* **2007**, *111*, 13794−13803.
(38) Sinha, G.; Depero, L. E.; Alessandri, I. Recyclable SERS Substrates Based on Au-Coated ZnO Nanorods. *ACS Appl. Mater. Interfaces* **2011**, *3*, 2557−2563.
(39) Alessandri, I.; Depero, L. E. Metal Oxide Microrings with Femtoliter Capacity for Raman Microspectroscopy. *ACS Appl. Mater. Interfaces* **2010**, *2*, 594−602.
(40) Wang, L.; Zhu, Y.; Xu, L.; Chen, W.; Kuang, H.; Liu, L.; Agarwal, A.; Xu, C.; Kotov, N. A. Side-by-Side and End-to-End Gold Nanorod Assemblies for Environmental Toxin Sensing. *Angew. Chem., Int. Ed.* **2010**, *49*, 5472−5475.
(41) Stewart, A. F.; Lee, A.; Ahmed, A.; Ip, S.; Kumacheva, E.; Walker, G. C. Rational Design for the Controlled Aggregation of Gold Nanorods via Phospholipid Encapsulation for Enhanced Raman Scattering. *ACS Nano* **2014**, *8*, 5462−5467.
(42) Lyvers, D. P.; Moon, J.-M.; Kildishev, A. V.; Shalaev, V. M.; Wei, A. Gold Nanorod Arrays as Plasmonic Cavity Resonators. *ACS Nano* **2008**, *2*, 2569−2576.
(43) Khatua, S.; Paulo, P. M. R.; Yuan, H.; Gupta, A.; Zijlstra, P.; Orrit, M. Resonant Plasmonic Enhancement of Single-Molecule Fluorescence by Individual Gold Nanorods. *ACS Nano* **2014**, *8*, 4440−4449.
(44) Park, K.; Drummy, L. F.; Wadams, R. C.; Koerner, H.; Nepal, D.; Fabris, L.; Vaia, R. A. Growth Mechanism of Gold Nanorods. *Chem. Mater.* **2013**, *25*, 555−563.

DOI: 10.1021/acsami.5b07175
ACS Appl. Mater. Interfaces 2015, 7, 18794−18802